Development of Inductive Oil Debris Sensors for Wind Turbine Gearboxes

Christopher M. Allison, Christopher J. Crabtree*
*School of Engineering and Computing Sciences, Durham University, UK
c.j.crabtree@durham.ac.uk

1. Introduction

Wind energy is central to UK and EU renewable energy production targets for 2020. However, the Levelised Cost of Energy needs to reduce from £140/MWh to below £100/MWh [1]. With operation and maintenance (O&M) costs accounting for up to 30% of the LCoE, there is a need for predictive and preventative maintenance strategies. Condition monitoring is at the heart of these. Wind turbine reliability is a major concern as the downtime associated with large mechanical components is significant [2]. Vibration measurements are traditionally used for gearbox monitoring however operators often lack confidence in results. Monitoring gearbox oil debris can provide a secondary signal to act as confirmation of any change in gearbox vibration.

However, many systems for oil debris monitoring cannot be incorporated into the main oil flow due to their small cross sectional areas and resulting pressure drops. Placing sensors in an offline loop removes the direct link to operational parameters. A continuous in-line measurement allows measurements to be correlated against operational parameters so that fault responses can be isolated.

This paper presents work on non-intrusive, continuous oil debris monitoring sensors based on inductive coils. The paper introduces the background theory and simulations, sensor development, and test results.

2. Approach

Current technologies involving inductive sensing principles, based on single coil solenoids have been used to analyse the health of F22 fighter jet engines [3] by monitoring disturbances to an alternating magnetic field. This paper investigates the coil configuration and sensing methods. The test section radius was sized to replicate a WT lubrication system.

An oil circulation system was installed for online testing and will be described in the final paper.

2.1. Theory and Method

The principle of detecting non-ferrous and ferrous metal debris in fluid flow is shown in Figure 1. An AC current flows through a coil wound around a pipe with oil ($\mu_r \approx 1$) flowing through it (Figure 1(a)). If a metal particle passes through the pipe, two factors affect the coil inductance [4]:

- Relative magnetic permeability change (equation (1)).
- Eddy currents acting to oppose the magnetic field [4].

$$L = \frac{\mu_0 \mu_r N^2 \pi r^2}{l} \qquad (1)$$

where L is coil inductance (H), μ_0 is permeability of free space ($4\pi \times 10^{-7}$), μ_r is core relative permeability, N is the number of turns, r is the radius (m) and l is the solenoid length (m).

Ferrous particles increase the effective inductance (Figure 1(b)) as $\mu_r \gg 1$, dominating any counteracting eddy current effects [5]. In comparison, eddy currents from non-ferrous particles dominate and coil inductance decreases (Figure 1(c)). [6] confirmed that higher excitation frequencies cause larger eddy currents and inductance drops. Thus, ferrous and non-ferrous particles and their size can be differentiated.

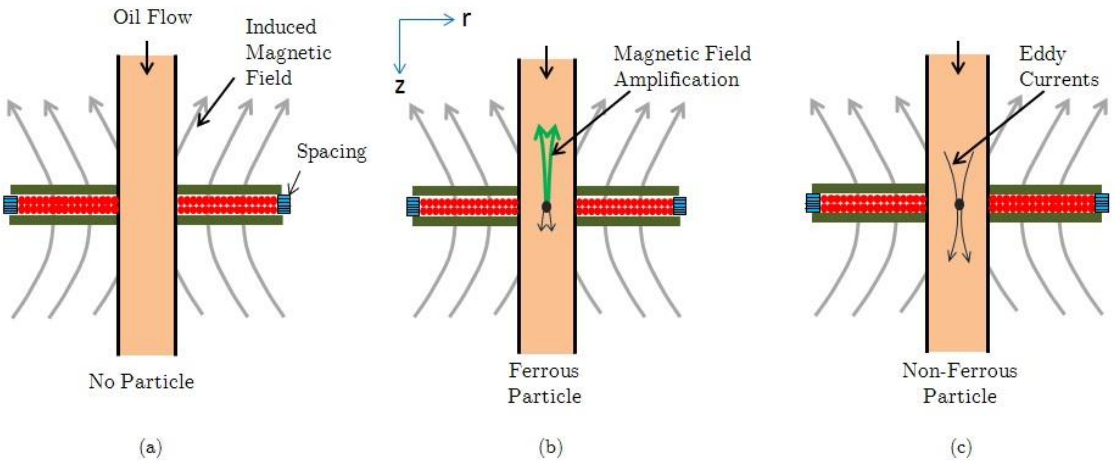

Figure 1: Inductive planer coil sensing principle. (a) Applied magnetic field. (b) Magnetic flux enhanced by a ferrous particle. (c) Magnetic flux attenuated by eddy currents.

Table 1: Coil design parameters

Coil Type	No. of Turns	No. of Layers	Length (mm)
Short Solenoid	40	2	12.0
Long Solenoid	80	1	26.0

2.2. COMSOL Optimisation and Design

Initial work modelled the sensor designs using COMSOL Multiphysics to optimise coil parameters. The resulting parameters for manufacture included:

- Test section outer diameters of 8mm, 10mm and 15mm fitting with real system pipe sizes [7].
- Two layers of turns for the short solenoid, planar coil and three coil setup for improved sensitivity.
- Winding wire diameter of 0.21mm to concentrate turns.

A three-coil approach using two excitation coils and a sensing coil was also taken based on COMSOL simulation. The outer coils are wound in opposite directions so that the magnetic field from each cancels at the centre of the sensing coil (Figure 2), producing a region that is highly sensitive to weak disturbances. Particle passing through the first field coil bias the field in the zero region resulting in an output signature in the sensing coil [8]. The signal phase is opposite for ferrous and non-ferrous material and the amplitude depends on the mass and surface area respectively [9].

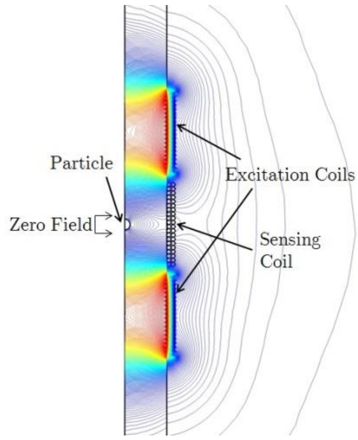

Figure 2: Contour plot of magnetic field in the sensing coil.

A frequency sweep in COMSOL validated that the change in inductance indicates the material present (Figure 3) and a frequency of 200kHz allows differentiation between materials.

An LC resonance circuit was matched with the sensing coils, according to (2) at 200kHz.

$$C_p \approx \frac{1}{4\pi^2 f_r^2 L_s} \qquad (2)$$

where C_p is the external capacitor (F), f_r the resonant frequency (Hz) and L_s the measured coil inductance (H).

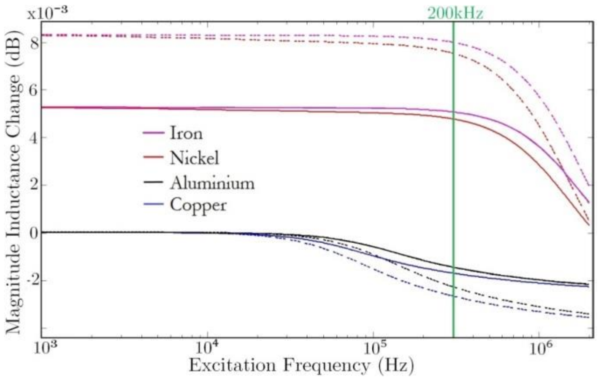

Figure 3: Bode plot of 8mm (dashed) and 12mm (solid) diameter short solenoids.

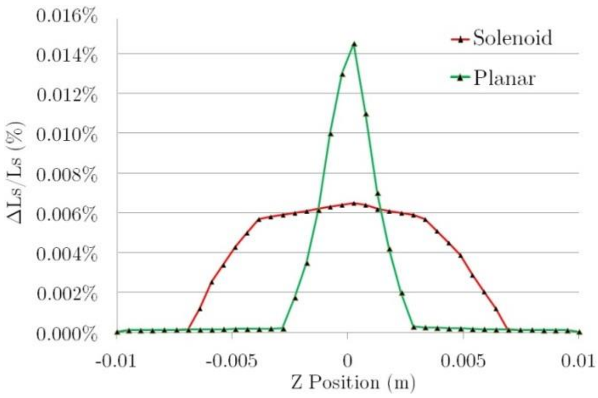

Figure 4: Relative inductance change as a function of particle radial position.

3. Results and Discussion

3.1. COMSOL Particle Position

COMSOL was used to analyse the effect of particle radial position within the sensing region of each coil configuration. The solenoid configuration was least sensitive to radial position (Figure 4). However, flow should be kept as consistent as possible to reduce turbulent particle movement.

3.2. Coil Performance

Physical sensors were tested at their resonant frequencies using a range of different particles to demonstrate coil sensing capabilities. Figure 5 shows one experimental run for the short solenoid configuration. The pairs of peaks correspond to a particle being inserted and removed. From left to right, the particles are:

- **Iron:** 0.5mm, 1mm, 2mm
- **Aluminium:** 1mm, 2mm
- **Steel:** 1mm, 3mm

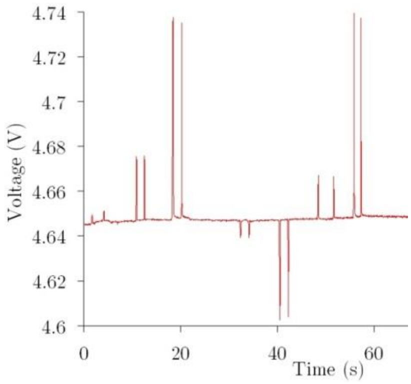

Figure 5: 8mm short solenoid debris test.

Testing found that:

- The coils could not detect 0.5mm diameter aluminium particles.
- There is a positive and consistent correlation between particle size and disturbance signal magnitude.
- Ferrous and non-ferrous materials can be differentiated by the polarity of the voltage change.
- The most successful coil configuration was the 8mm diameter short solenoid with significantly larger voltage changes than other configurations.
- The test section diameter should be minimised.
- An increased turns density (N/l) produces a more sensitive design.

To identify the minimum detectable particle size, debris in oil was introduced to the test section. This showed a detection limit of 420µm for iron and 900µm for aluminium particles, where both particle signatures were 1.5mV and close to being lost in noise.

Results showed interaction between particles affect detection peaks. When consecutive particles were of different materials, the disturbance signals were attenuated but it was still possible to identify that two particles had passed and the order in which they had passed.

3.3. Three Coil Concept

To validate the theoretical benefits of the three coil design (see Figure 2) the most successful parameters from the previous analysis were selected. Three short, two-layer solenoids with 40 turns were wound onto 8mm test sections with coil spacing of 1.5mm.

Debris test results for the single and three-coil configurations are outlined in Table 2. The amplified detection is critical to improving the detection limits because detection of smaller particles indicates the first stages of wear. This design was able to detect smaller particles (280µm iron and 750µm aluminium).

Table 2: Three coil comparison vs single coil

Particle Type	Single Coil Voltage Change (V)	Three Coil Voltage Change (V)	% Change
ø0.5mm Iron	0.0033	0.016	380%
ø1mm Iron	0.028	0.126	350%
ø2mm Iron	0.0823	0.336	308%
ø1mm Al	-0.0073	-0.0425	480%
ø2mm Al	-0.0407	-0.121	198%

4. Conclusions

This paper has demonstrated:

- Inductive oil debris sensors using high-frequency resonance circuits can be used to detection ferrous and non-ferrous particles in oil.
- Single inductive coils were able to differentiate particles of 450µm for iron and 900µm for aluminium.
- A three coil design improved particle detection limits to 280µm for iron and 750µm for aluminium.

The full paper will show results from the oil circulation test rig to demonstrate the sensing principles apply in an operational environment.

Acknowledgements

This work was funded by the Durham Energy Institute EPSRC Impact Acceleration Account.

References

[1] E. Davey and A. Nimmo. Offshore Wind Cost Reduction, Pathways Study. 2012; http://www.thecrownestate.co.uk/media/305094/offshore-wind-cost-reduction-pathwaysstudy.pdf.

[2] F. Spinato, et al., Reliability of wind turbine subassemblies. Renewable Power Generation, IET, 2009. 3(4): p. 387-401.

[3] J. Miller and D. Kitaljevich, “In-line oil debris monitor for aircraft engine condition assessment,” in Aerospace Conference Proceedings, 2000 IEEE, vol. 6, 2000, pp. 49–56 vol.6.

[4] L. Du and J. Zhe, “A high throughput inductive pulse sensor for online oil debris monitoring,” Tribology International, vol. 44, no. 2, pp. 175–179, 2011.

[5] D. Sokolov et al., “Metal separator for copper and stainless steel,” 2012.

[6] L. Bendong et al., “Research on the influence of excitation frequency on the sensitivity in metal debris detection with inductor sensor,” Advances in Mechanical Engineering, vol. July 2014.

[7] Kittiwake, On-Line Sensor Brochure. Kittiwake Development Ltd, 2013.

[8] C. Li, J. Peng, and M. Liang, “Enhancement of the wear particle monitoring capability of oil

debris sensors using a maximal overlap discrete wavelet transform with optimal decomposition depth," Sensors (Basel, Switzerland) 14. 4, vol. 4, Mar. 2015.

[9] D. M. Muir and B. Howe, "In-line Oil Debris Monitor (ODM) for the Advanced Tactical Fighter Engine. SAE Paper 961308, May 1996.

[10] F. Zhang et al., "Research on the detection of metal debris with micro inductive sensor embedded in lubricant." Journal of Chemical and Pharmaceutical Research, vol. 6, no. 7, pp. 2249–2254, 2014.